WCTE 2014 Quebec City Canada August 10-14
World Conference on Timber Engineering

# EVALUATION ON DYNAMIC PERFORMANCE OF GLULAM FRAME STRUCTURE COMPOSED OF SLOTTED BOLTED CONNECTION SYSTEM

**Kohei Komatsu[1] , Takuro Mori[2], Akihisa Kitamori[3], Yasuhiro Araki[4]**

**ABSTRACT:** Earthquake-resisting performance of glulam frame structure was evaluated by shaking table tests on a specially designed glulam "double cross shape" specimen composed of slotted bolted connection (SBC) system. By the first vibration test using sinusoidal wave having a maximum acceleration of 800gal, the specimen survived until 80% level of input waves without damage. After renewing SBC system, the second vibration test was done on a same specimen using the JMA-Kobe NS waves having a PGA of 818gal. The specimen survived until 80% level of input without damage but slightly failed by the panel-shear when 100% level was inputted. Earthquake-resisting performance of glulam moment-resisting joints composed of SBC system was considered as satisfactory enough for ductile joint system, but improvement of panel-shear of glulam member itself was recognized as a future research need.

**KEYWORDS:** Slotted bolted connection (SBC), Glulam portal frame, Lagscrewbolt (LSB), Panel shear failure

## 1 INTRODUCTION

In Japan, it is certainly anticipated that large scale public buildings made of timber will increase due to the good wind blow by "Law for Promoting Large Scale Wooden Public Building" enforced in May 2010. Japan, however, is one of the most earthquake prone countries in the world thus it is urgent requirements for us to develop earthquake resisting large scale wooden buildings.

In this study, we aimed to develop a moment-resisting joint for glulam portal frame structure, which can behave as rigid as possible during initial deformation level before yielding, after once some joint reaches to its yielding point, it can deform as ductile as possible by making use of the friction resistance of steel joint plus some amount of steel-to steel embedment resistance based on the idea of conventional Slotted Bolted Connection (SBC) technique. In addition to these, once devastating earthquake is over, the deformed structure can be easily restored into the original form by releasing a several high tension bolts and if necessary by replacing steel side plates with new ones at deformed joints. Furthermore, in this study, we intended to realize these several performances with low cost method by modifying a little bit on conventional glulam joints techniques.

[1] Kohei Komatsu, RISH, Kyoto University
Gokasyo, Uji, 611-0011 Japan
Email: kkomatsu@rish.kyoto-u.ac.jp
[2] Takuro Mori, Kyoto University, Japan
[3] Akihisa Kitamori, Kyoto University, Japan
[4] Yasuhiro Araki, Building Research Institute, Japan

## 2 PREVIOUS RESEARCHES

It is likely to be back in 1976 that the earlier researches on SBC has started [1], but the first scientific research which gave the great effects on the practical application of this method for actual steel construction field might be that of Grigorian, Yang and Popov [1] published in 1993. It was estimated that they completed a reasonable and economical friction damper system for steel framed buildings by using SBC technique [2],[3]. They used "1/8" thick UNS-260 half-hard cartridge brass plate" between main and side steel plate as well as Belleville washer (8-EH-112 Solon compression hardened washer) for ensuring stable Coulomb friction hysteresis loops. The first application of SBC technique to timber connection was done by Duff et al. [4] in US. Unfortunately, as the details of connection they designed and the experimental procedures were also not described clearly, we could not know how actually SBC acted on moment-rotation relationship in a kind of moment resisting column-beam joint. In Japan, Araki et al. [5] applied SBC technique to a special bolted moment-resisting glulam joint.

We have developed a ductile moment-resisting joint system successfully by making use of SBC idea with slightly adding our own originality which to be explained in latter section more in details [6] and its static performance was reported at WCTE2012 in Auckland, NZ [7]. In this study, dynamic performances of moment-resitting joints in partial two storey frame structure composed of new joint technique were evaluated by using shaking table experiments.

## 3 EXPERIMENTS

### 3.1 TEST SPECIMEN

Figure 1 shows a conceptional diagram of a "double cross-shape" specimen, which was designed to simulate approximately linked behaviours of beam-column joint and column-leg joint within a one compact specimen by picking up of 1/8 part of 2 storey and 5 rows virtual glulam portal frame structure of 8m by 6m floor area.

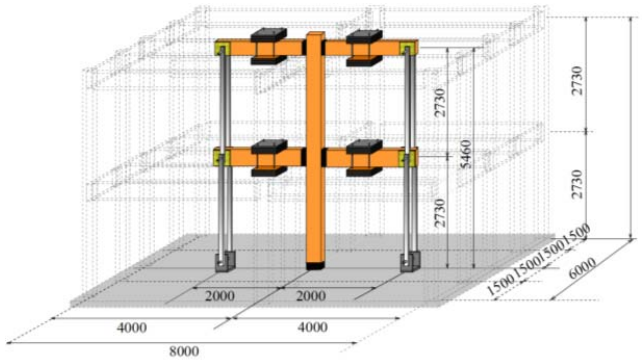


***Figure 1*** *:"Double cross-shape" specimen*

Figure 3 shows details of double cross shape test specimen with weights and various measuring devise.

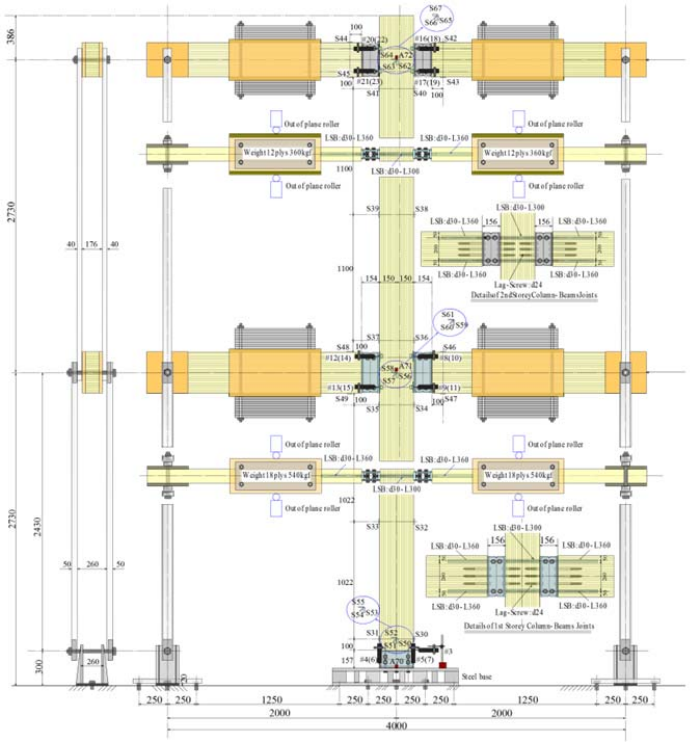

***Figure 3 Details of double cross shape specimen.***

Strain gauges S30 to S49 (20mm gauge length) were attached at both sides of beam and column members to measure the bending moments at beam-column as well as column-leg joints. While rosette gauges S50 to S67 (20 mm gauge length) were attached on the both surfaces of panel zone of each layer to measure the panel shear strains. Rotational angles of each moment-resisting joint were measured using pair of high precise deformation measuring devices (±25mm gauge length) #4 & #5 to #22 & #23 for estimating moment-rotational relationships of each moment-resisting joint.

Storey drifts of double cross shape specimen were measured by using wire-type measuring devices ( ± 250mm gauge length) of #1 and #2. Horizontal deformation of leg joint was measured by using 50 mm high precise measuring devise #3.

Inertia force of each layers were measured by using acceleration meters (one directional 2G capacity) of A70 to A72 fixed on column member using double coated tape.

Figure 3 shows an actual feature of test set-up of "double cross shape" specimen on a shaking table facility.

***Figure 3*** *:Test set-up of specimen on a shaking table.*

Glulam members used were all European red-pine of JAS E105-F300 grade. For 2nd storey beams, 120mm×300mm cross sectional glulam was used. While for 1st storey beams, 120mm ×360mm cross sectional glulam was used. For a column, 120mm×300mm cross sectional glulam was used.

### 3.2 JOINT DETAILS

Figure 4-(a) and (b) show details of beam-column and column-leg joint, respectively. In both joints, 9mm thickness SS400 steel was used to make U-shape main element and 6mm thickness SS400 steel was used for slotted splice plates. Main U-shape steel element and slotted splice plates were assembled with F10T-M16-High Tension Bolts accompanying with double Belleville

washers per bolt for preventing sudden drop of tightening force [1].

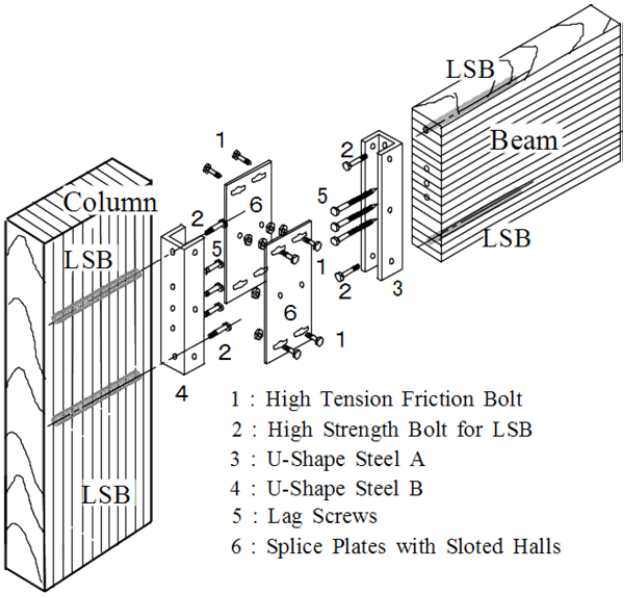


*(a) beam-column joint*

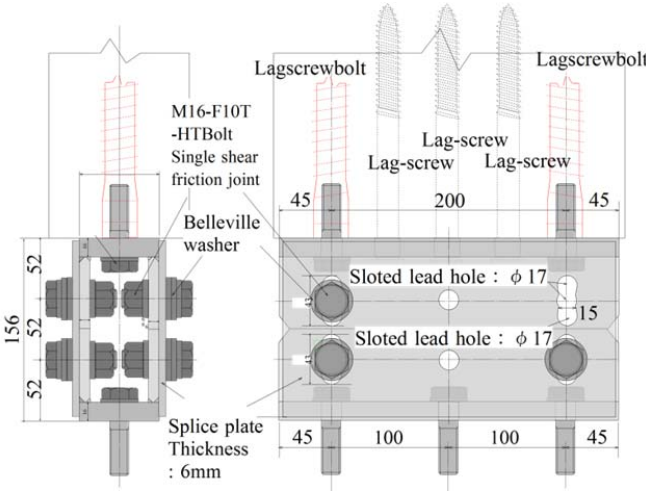


*(b) column-leg joint*

***Figure 4**: Details of Joints*

Lagscrewbolts® (hereafter denote as LSB) having crest diameter of 30mm and penetrating length of 300mm were used perpendicular to the grain so as to transverse in the column member at first and second storey beam-column joints. While LSBs with crest diameter of 30mm and penetrating length of 360mm were used parallel to the grain in beams as well as in column-leg joint.
Figure 5 shows a photo of LSBs same type as used in this experiment.

***Figure 5** Photo of LSB same type as used in this study.*

According to our design standard on LSB joints, LSB is considered to resist against only for axial force. While for resisting against shear force, we assumes that other different resisting elements should correspond to shear force. In this study, therefore, we assumed that shear force could be resisted by conventional lag-screws with diameter of 24mm. Figures 6-(a) to (d) are photos showing preparation of LSB joint and built-up of double cross shape specimen.

*(a) Penetrating lag-screws for shear (previous experiments)*

*(b) Measuring devices* *(c) Rosette gauges*

*(d) Acceleration meter* *(e) Lateral roller support*

***Figures 6** Built-up LSB joint and double cross specimen.*

### 3.3 ADDITIONAL WEIGHT FOR SHAKING TABLE TEST

Weight used for the calculation of earthquake force was estimated on the original 2 storey 5 bays glulam portal frame structure by assuming following unit values;
1) Roof: Steel plate (t=0.5mm) with purlin and lath board = 0.7kN/m$^2$
2) Wall: 0.55 kN/m$^3$
3) Floor: Thick plywood (t=28mm)=0.7kN/m$^2$
4) Balcony: 0.65 kN/m$^3$
5) Live load (earthquake) :0.6kN/m$^2$
6) Floor area : 6m × 8m
7) Roof area : 6.8m × 8.8m

8) Glulam member: 1st storey beam=120mm × 360mm, 2nd story beam=120mm × 300mm, all column =120mm × 300mm, density=4.3 kN/m$^3$
9) Storey height: 2.73m

By taking the above mentioned unit loads into account of assumed 2 storey 5 bays building, we got the following total weight for each storey by eliminating beam and column weight.

1st storey =84.81kN
2nd storey=56.44kN

As the double cross specimen was assumed to be picked-up from 1/8 area of global plane area,

1st storey =84.81/8=10.6kN
2nd storey=56.44/8=7.055kN

Thus finally, for the half side of the 2nd storey beam, a weight of 0.36tf and for the half side of the 1st storey beam, a weight of 0.54tf was distributed respectively as the additional weights for shaking table test using double cross shape specimen.

### 3.4 INPUT WAVES AND SHAKING SCHEDULE

Two different kinds of waves were employed for shaking table tests.
The first wave used was a sinusoidal wave having a 2Hz frequency, ±50mm maximum amplitude, and maximum acceleration of 800gal.
The second wave used was the JMA-Kobe NS component recorded waves with maximum acceleration of 818gal.
Shaking schedule is shown in Table.1.

Table1 Shaking schedule

| | First series | | Second series |
|---|---|---|---|
| 1 | Sinusoidal wave 20% | 6 | JMA-Kobe-NS 20% |
| 2 | Sinusoidal wave 40% | 7 | JMA-Kobe-NS 40% |
| 3 | Sinusoidal wave 60% | 8 | JMA-Kobe-NS 60% |
| 4 | Sinusoidal wave 80% | 9 | JMA-Kobe-NS 80% |
| 5 | Splice plates with slotted holes, high-tension-bolts were replaced by new sets | 10 | JMA-Kobe-NS 100% |
| | | 11 | JMA-Kobe-NS 120% |
| | | 12 | Sinusoidal wave 100% |

From preliminary response analysis, as it was found out that in the level of sinusoidal wave 100% input, panel shear stress criteria at 1$^{st}$ storey beam-column joint might become critical, thus the input of sinusoidal wave 100% was postponed to the last of all experiments, and as shown in the stage 5 of the Table 1, splice plates with slotted holes and high-tension-bolts were all replaced by new sets of them to simulate the situation for restoring beam-column and column-leg joints from damage due to devastate earthquake attack.

## 4 ANALYSES

### 4.1 HYSTERESIS MODEL FOR JOINTS

In our previous studies [6,7], although we used NCL model developed by Tani et al[8] for predicting static behaviours of column-beam joints or/and column-leg joint, in this dynamic research stage, however, we selected the modified Ramberg-Osgood model[9] as an alternative hysteresis model because a problem in the optional part of computer program of NCL hysteresis model was found out. For the skeleton curve, we used tri-linear polygonal relationship whose yielding value and initial stiffness were determined by the design equation for the high-tension bolt [10] and mechanical model on steel joint part [6,7]. While for the secondary or third stiffness and ultimate load carrying capacity were determined by the experimental values on the beam-column or/and column-leg joint [6,7].
For the parameters of Ramberg-Osgood model which dominate hysteretic characteristics in loading and unloading loops, so-called try-and-error method was used so as to fit the model curve well with experimental hysteresis curves of static push-pull cyclic test data [6,7].

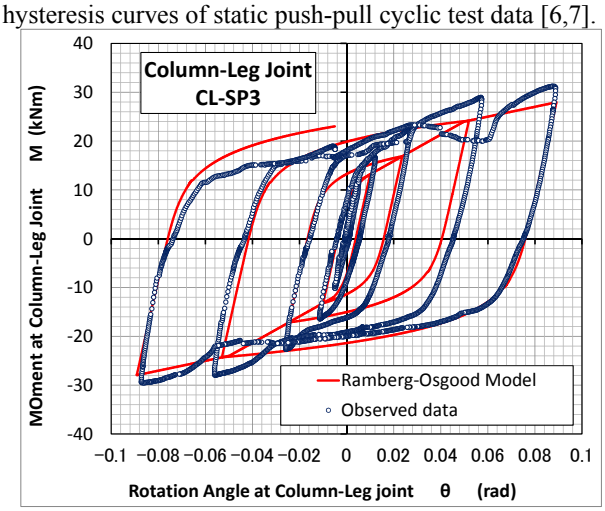


*(a) Column-Leg Joint [6,7]*

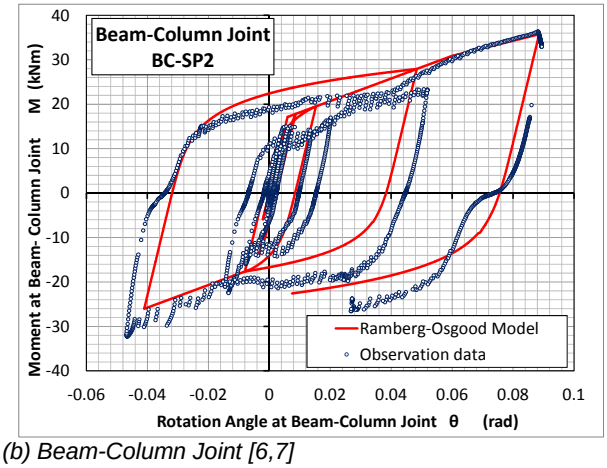


*(b) Beam-Column Joint [6,7]*

***Figure 7*** *Comparisons between observed moment-rotation relationships and predictions by Ramberg-Osgood model subjected to static push-pull cyclic load.*

Figures 7-(a) and (b) show comparisons between observed moment-rotation relationships and predicted ones by Ramberg-Osgood model. Parameters for executing numerical calculation of Ramberg-Osgood model are tabulated in Table 2.

Table 2 Parameters for Moment-Rotation Relationship used in Ramberg-Osgood model.

| | $R_J$ | $M_c$ | $M_y$ | $\alpha$ | $\beta$ | p1 | p2 |
|---|---|---|---|---|---|---|---|
| | kNm/rad | kNm | | | | | |
| Beam-Column | **1724** | **13.22** | **24.50** | **0.113** | **0.061** | **0.001** | **10** |
| Leg-Column | **2147** | **12.00** | **23.97** | **0.126** | **0.047** | **0.001** | **10** |
| Cross Beam-Column | **1605** | **10.17** | **17.00** | **0.097** | **0.016** | **0.001** | **10** |

*Remarks*: p1, p2 are implicit hysteresis parameters to control the form of nonlinear hysteresis loops used in computer program.

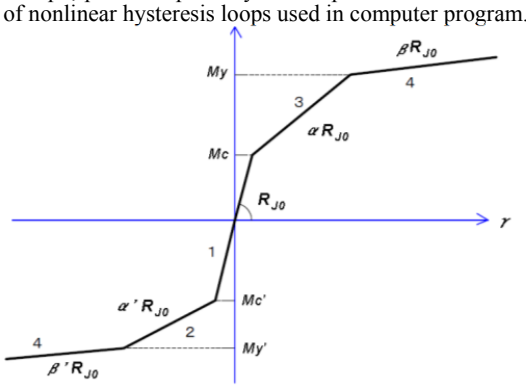


## 4.2 RESPONSE ANALYSES

We used so-called Newmark-β method (β=0.25) for analysing all time history response analyses by making use of a commercial computer program named as SNAP-Ver.6[10]. Time interval of numerical calculation used was 0.01second at most analyses. Dumping ratio used was 0.02.

## 4.3 RELIABILITY OF USING DOUBLE CROSS SHAPE SPECIMEN

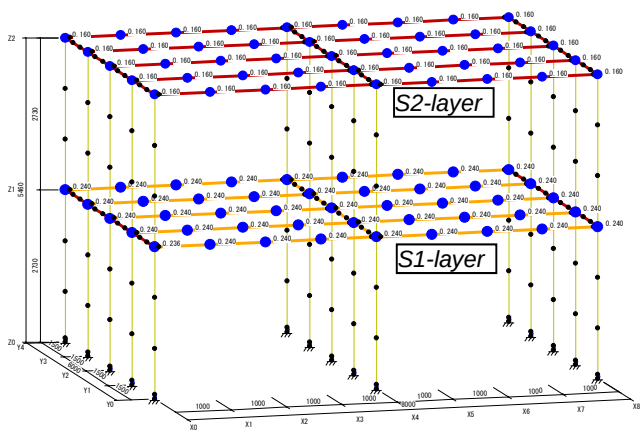


*a) Original 5 bays 2-storey building 3D- FEM model*

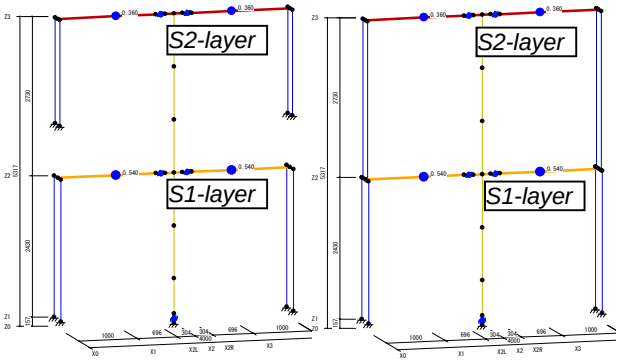


*b) Approximate model* *c) Quasi-Approximate model*

***Figure 8*** *Three FEM response analyse models*

At first, we show comparisons among computed results of three different models to ensure the reliability of using double cross shape specimen (*Quasi-Approximate model*). It is natural to use Fig.8-b) "Approximate model" if we chose an approximate model to investigate partial behaviour of beam-column or/and column-leg joint subject to shaking input instead of Fig.8-a) "Original model". The test set-up of "Approximate-model", however, required fairy rigid supporting system on shaking table. Thus we examined applicability of Fig.-c) "Quasi-Approximate model" as the next best choice of the model-a).

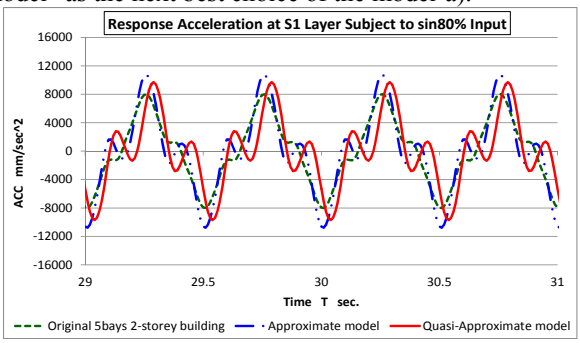


*a) Response accelerations at S1-layer with sin 80% input*

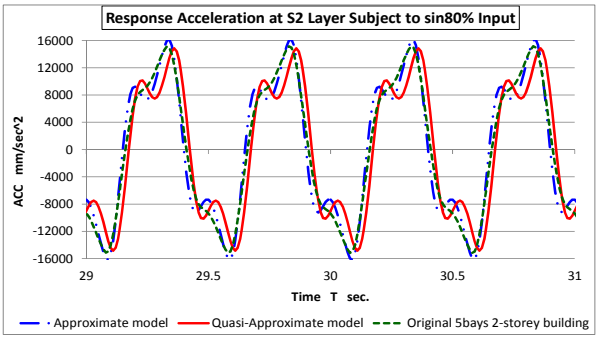


*b) Response accelerations at S2-layer with sin 80% input*

***Figure 9*** *Comparisons of response accelerations.*

Figures 9-a) and-b) compare response acceleration of three different models by inputting the same sinusoidal wave of 80% amplitude. It is very interesting to see that in spite of the fact that three FEM models having different configurations and boundary conditions but they showed almost same peculiar kinked responses. This kinked

response might be interpreted by the effect of higher order vibration modes.

Figure 10-a) and-b) compare response moments at column-leg joint as well as beam-column joint at S1-layer of three different models by inputting the same sinusoidal wave of 80% amplitude. In cases of moment response, no more kinked form responses are seen. From these comparisons, the reliability of using "Quasi-Approximate model =Double Cross Shape Specimen" was ensured.

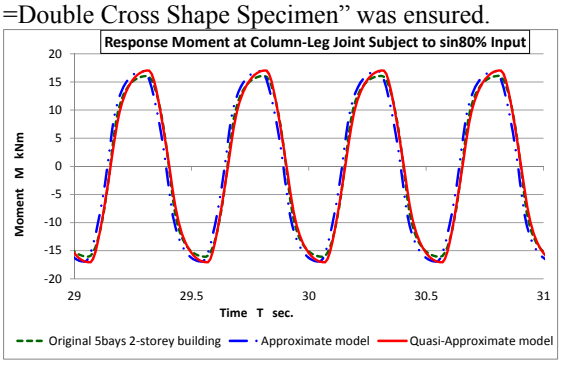


*a) Response moment at column-leg joint*

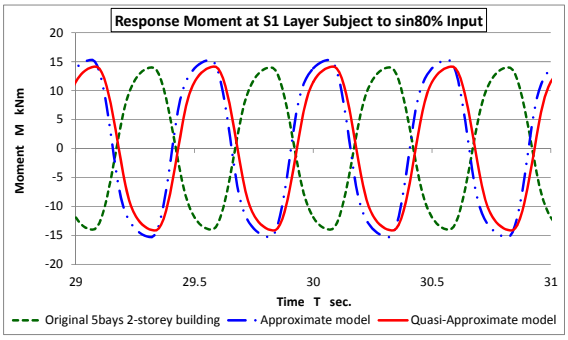


*b) Response moment at beam-column joint at S1-layer.*

***Figure 10:*** *Comparisons of response moments.*

## 5 RESULTS AND DISCUSIONS

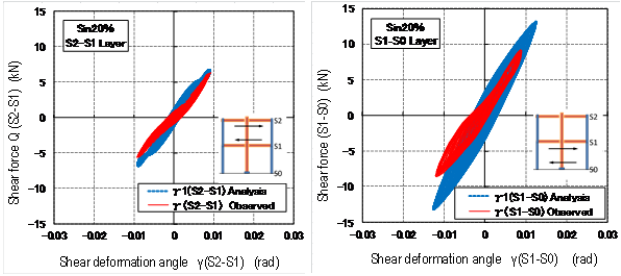


*a) Force-shear deformation angle at 20% sin wave input.*

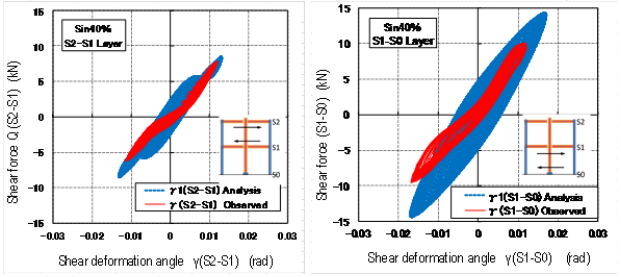


*b) Force-shear deformation angle at 40% sin wave input. (blue: analysis red: observation)*

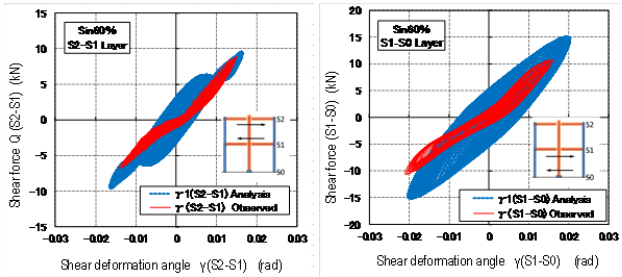


*c) Force-shear deformation angle at 60% sin wave input. (blue: analysis red: observation)*

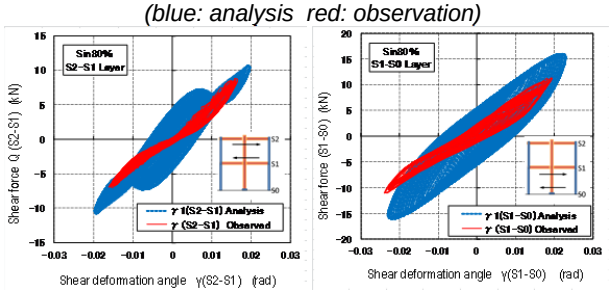


*d) Force-shear deformation angle at 80% sin wave input. (blue: analysis red: observation)*

***Figures 11*** *Comparisons between analyses and observations subject to sinusoidal waves from 20 to 80%.*

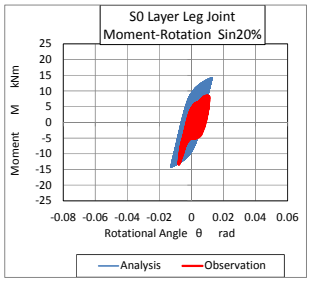


*a) 20% sin wave input*

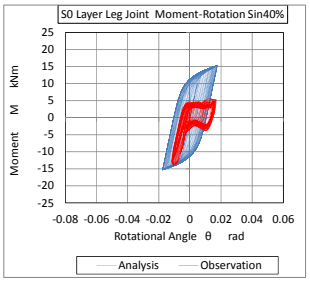


*b) 40% sin wave input (blue: analysis red: observation)*

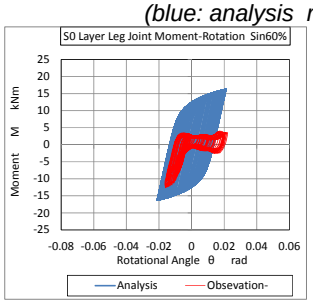


*c) 60% sin wave input*

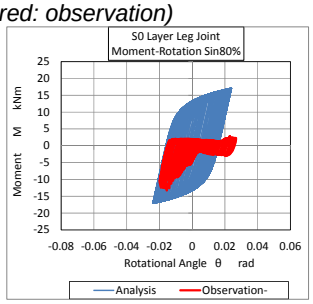


*d) 80% sin wave input (blue: analysis red: observation)*

***Figure 12*** *Progresses of eccentric response at column-leg joint as increase of input amplitude level. Blue lines indicate analyses and red ones indicate observations.*

Figures 11-a) to d) show comparisons of shear force-shear deformation angle relationships obtained by response analyses and experimental observations in case of sinusoidal waves inputs from 20% till 80% amplitude. It was found that observed responses did not show fat loops nor larger response while analytical results showed fairy fat loops and larger response. These discrepancies seem to be caused by drop of rigidity at leg-joint due to loss of contact pressure at HTB by abrasions on contact surface of

steel splice plates as shown in Figure 13 due to so many times cyclic frictions.

***Figure 13*** *Abrasive marks on the contact surface of splice plate near slotted bolt holes caused by 480 cycle's frictions.*

Actually, cyclic motion by sinusoidal wave having 2Hz frequency acting 60 seconds gives 120 cycles frictions. Therefore, one side HT-bolted joint at column-leg joint seems to lose its original performance at first series of input by sin 20% amplitude as can be deduced from Figs. 12-a) to d) which show progresses of eccentric moment-rotational relationship observed at column-leg joint.

After the test using sinusoidal wave of 80 % amplitude, splice plates, high-tension bolts and Belleville washers in all joints were replaced by the new sets. Figures 14-a) to g) show comparisons between response analyses results and observed ones in case of JMA-Kobe NS waves from 20% till 120% amplitude and additional sin100% input.

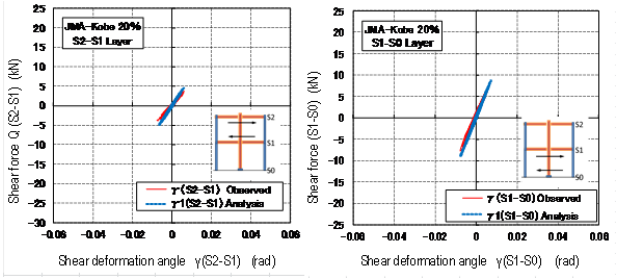


*a) Force-shear deformation angle at 20% JMA-Kobe input.*

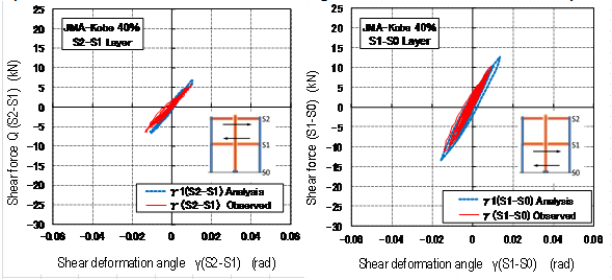


*b) Force-shear deformation angle at 40% JMA-Kobe input.*

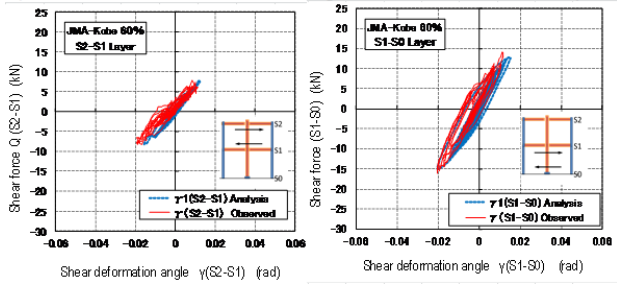


*c) Force-shear deformation angle at 60% JMA-Kobe input.*
*(blue: analysis red: observation)*

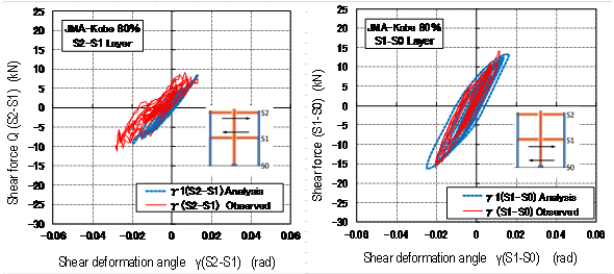


*d) Force-shear deformation angle at 80% JMA-Kobe input.*

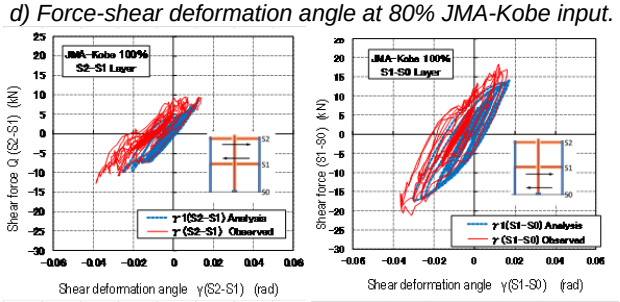


*e) Force-shear deformation angle at 100% JMA-Kobe input.*

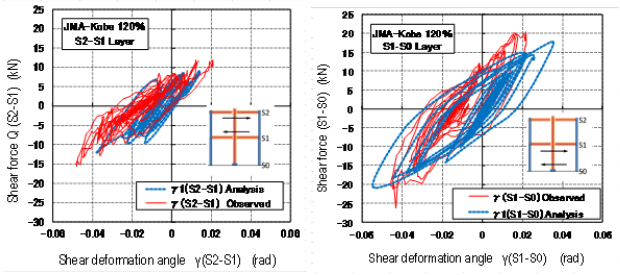


*f) Force-shear deformation angle at 120% JMA-Kobe input.*

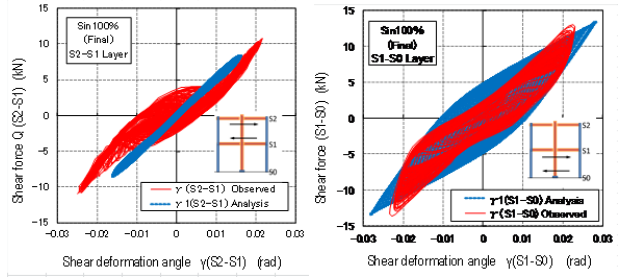


*(blue: analysis red: observation)*
*g) Force-shear deformation angle at 100% sin wave input.*

***Figure 14*** *Comparisons between analyses and observations subject to JMA-Kobe NS waves from 20 to 120% and additional sinusoidal wave 100% .*

In the case of JMA-Kobe NS wave inputs, agreements between analyses and observations were fairly well. This may be explained by the reason that less numbers of cyclic frictions compared with sinusoidal wave inputs were given to steel splice plates thus the decrease of holding power of HTB was relatively less hence anticipated performance was obtained.

In fact, shaking table test using actual earthquake observed wave, total numbers of cyclic friction that splice plates experienced were less than 1/10 of those given by the sinusoidal input through 20% till 80% inputs.

While in the case of additional input using sinusoidal 100% wave, interpretation about discrepancies between

observed and analysed results is difficult as specimen had already small scale shear failure at the 1st storey column-beam panel zone during test subjecting to JMA-Kobe 100% input as shown in Figure 15.

***Figure 15*** *Small scale panel shear failure at the 1st storey column-beam joint (photo was taken after all test was finished so glulam was laid horizontally).*

The stresses state in panel-shear zone of column-beam cross joint of frame structure will be expressed like Figure 16 [11]. If we trace the stress acting in the panel zone of the column-beam joint at 1st storey of the double cross specimen subjected to JMA-Kobe NS wave 100% input, the following calculation will be done;

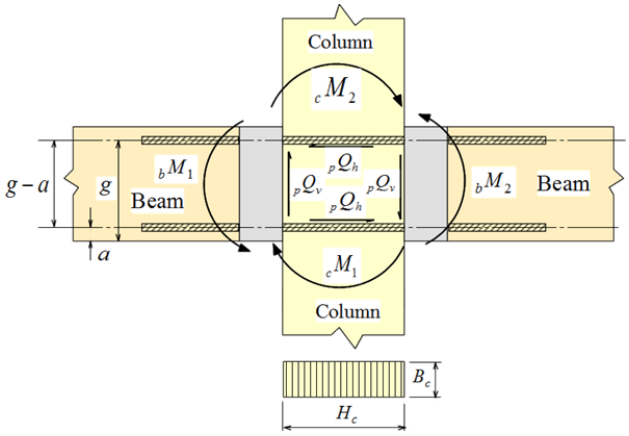


***Figure 16*** *Stress state in panel-shear zone [11].*

$$ {}_p\tau_v = \frac{{}_pQ_v}{B_c(g-a)} \le f_{ws} \qquad \ldots.(1) $$

$$ {}_pQ_v = \frac{|{}_cM_1 - {}_cM_2|}{H_c} \qquad \ldots.(2) $$

$$ {}_p\tau_h = \frac{{}_pQ_h}{B_cH_c} \le f_{ws} \qquad \ldots.(3) $$

$$ {}_pQ_h = \frac{|{}_bM_1 - {}_bM_2|}{g-a} \qquad \ldots.(4) $$

From the response analysis on the double cross shape specimen subject to JMA-Kobe NS waves 100% input, we got following maximum response stresses around panel zone;

At column element (C12 - C8) $ {}_cM_1 = 6.613\,\text{kNm}$

At column element (C8 - C4) $ {}_cM_2 = -32.03\text{kNm}$

At beam element (C6 - C7) $ {}_bM_1 = 16.0\text{kNm}$

At beam element (C9 - C10) $ {}_bM_2 = -16.0\,\text{kNm}$

$H_c = 300\text{mm}$

$B_c = 120\text{mm}$

$g - a = 200\text{mm}$

$F_{ws} = 3.0\text{N/mm}^2$ : Basic shear strength value of European red-pine [12]

$$ {}_p\tau_v = \frac{{}_pQ_v}{B_c(g-a)} $$

$$ = \frac{1000000 \times \frac{|6.613 + 32.03|}{300}}{120 \times 200} $$

$$ = \frac{128800}{24000} = 5.37 > F_{ws} = 3.0\text{N/mm}^2 \quad \text{NG} $$

$$ {}_p\tau_h = \frac{{}_pQ_h}{B_cH_c} $$

$$ = \frac{1000000 \times \frac{|16.0 + 16.0|}{200}}{120 \times 300} $$

$$ = \frac{160000}{36000} = 4.44 > F_{ws} = 3.0\text{N/mm}^2 \quad \text{NG} $$

As can be seen from the above mentioned calculations, the evaluated panel shear stresses caused by JMA-Kobe NS wave 100% input exceeded the assigned basic shear strength value of the European red-pine ($F_{ws}$=3.0N/mm$^2$) when the maximum response value was recorded. Therefore, it was actually recognized that the phenomena of shear failure at panel zone of 1st story column-beam joint was an important design criterion for this kind of glulam portal frame structure.

Figures 17-a) to g) show comparisons of moment-rotational angle relationship at column-leg joint or/and left-hand side column-beam joint at 1st storey obtained by response analyses and observations through strain gauges measurements in case of JMA-Kobe NS 20-120% input and final additional sinusoidal 100% input.

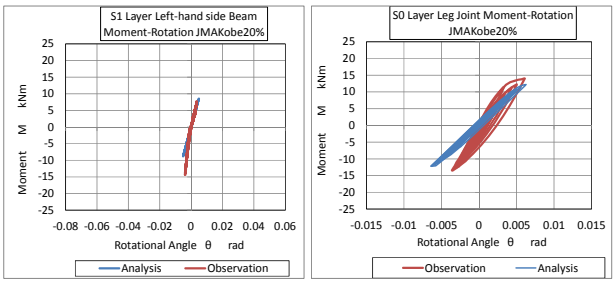


*a) Moment-rotational angle at 20% JMA-Kobe input. (blue: analysis red: observation)*

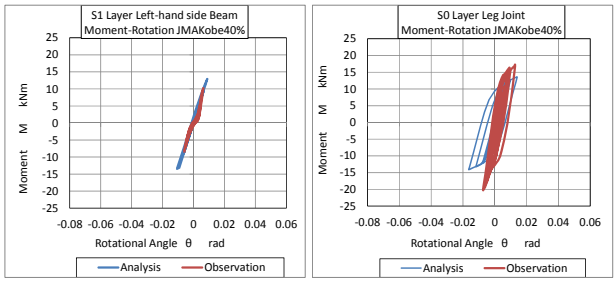


*b) Moment-rotational angle at 40% JMA-Kobe input. (blue: analysis red: observation)*

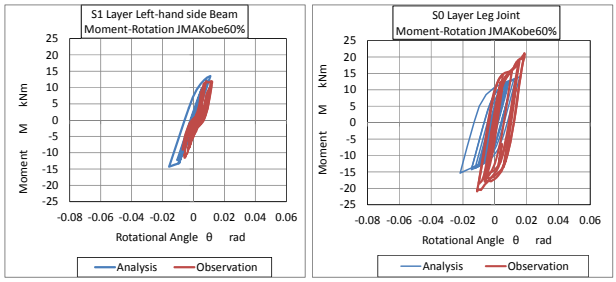


*c) Moment-rotational angle at 60% JMA-Kobe input. (blue: analysis red: observation)*

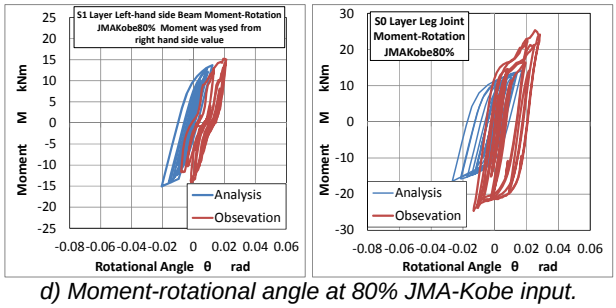


*d) Moment-rotational angle at 80% JMA-Kobe input. (blue: analysis red: observation)*

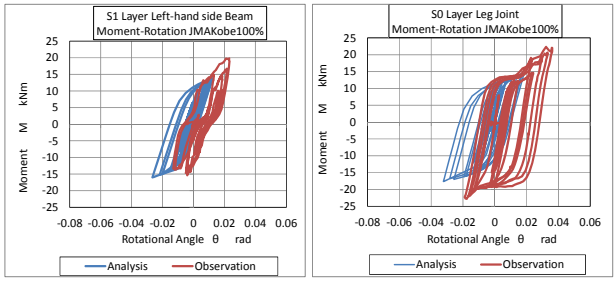


*e) Moment-rotational angle at 100% JMA-Kobe input. (blue: analysis red: observation)*

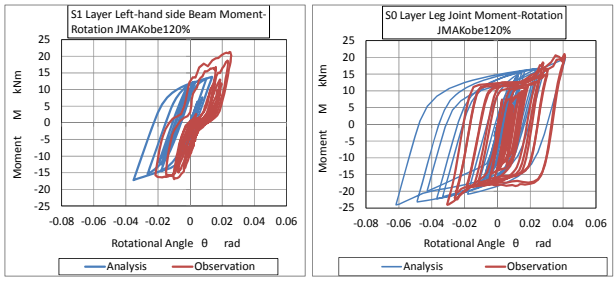


*f) Moment-rotational angle at 120% JMA-Kobe input. (blue: analysis red: observation)*

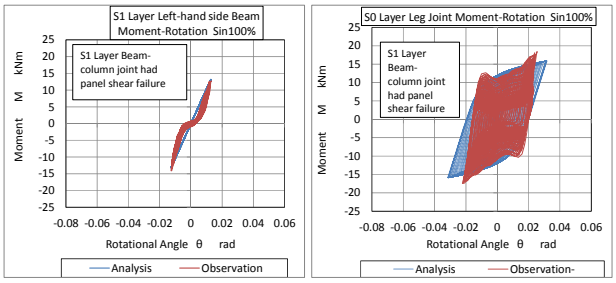


*g) Moment-rotational angle at 100% sin wave input. (blue: analysis red: observation)*

***Figure 17*** *Comparisons between analyses and observations subject to JMA-Kobe NS waves from 20 to 120% and final additional sin 100% .*

Generally speaking, it has been noticed that moment value determined by using measurement of strain gauge tended to show sometimes variances due to skill of strain gauge setting and effect of local timber properties. If considering such factors, analytical results on moment-rotational angle relationships showed same tendency as those measured at column-beam joint as well as column-leg joint.

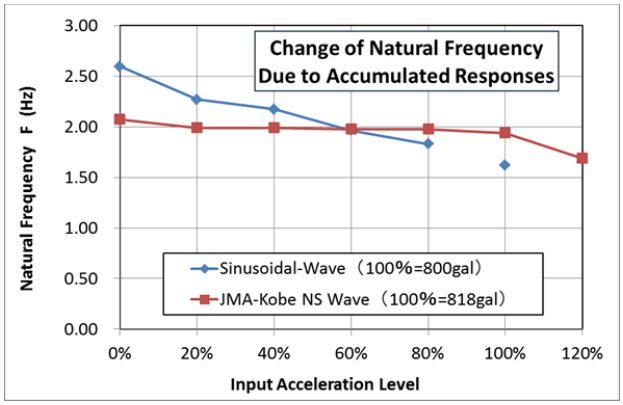


***Figure18*** *Change of natural frequency of the specimen*

Figure 18 shows change of natural frequency of the specimen through 2 different shaking table schedules. In the first series of test using sinusoidal wave, natural frequency of test specimen decreased from 2.598 Hz till 1.831Hz. The main reason of this decrease was thought to be caused by decrease of joint stiffness mainly due to the permanent slip of SBC system at column-leg joint.

***Figure 19*** *Permanent embedment deformation on the column side surface due to cyclic contact of steel box.*

After changing splice plates and others to new sets, the second series of test were continued by using JMA-Kobe NS waves. We expected that the natural frequency would recover to the original value by replacing damaged splice plates, but it returned back only to 2.07Hz. The differential value was thought to be caused by the permanent embedment deformation at the column side surface shown in Figure 19. For preventing this kind of embedment deformation, a method penetrating threaded long screws into the contact surfaces preliminary has been conformed to be effective [13].

## 6 CONCLUSIONS

Earthquake-resisting performance of glulam moment-resisting joints composed of SBC system was developed and their dynamic performance was evaluated by using double cross shape specimen subject to two different types of waves on shaking table test equipment. The following conclusions were obtained.

1. Energy dissipation mechanism developed showed preferable response for seismic input with JMA-Kobe NS wave.

2. Energy dissipation mechanism based on the slotted bolted connection system seemed not to be feasible against too many cycles of dynamic frictions. This conclusion was brought from the shaking table test subject to sinusoidal waves of 2Hz natural frequency with PGA of 800gal (actual inputs were given by 20, 40, 60, 80 and 100% amplitude) for 60 seconds input.

3. Numerical analyses using a commercial FEM program worked well for predicting nonlinear behaviour of glulam semi-rigid portal frame system composed of slotted bolt connection system as semi-rigid and ductile joints by modelling nonlinear moment-rotation relationship of each joint with Ramberg-Osgood formula.

4. Panel-shear failure will be important design criterion for this kind of glulam frame structures constituted of cross-shape column-beam joints

## ACKNOWLEDGEMENTS

This work was supported by Grants-in-Aid for Scientific Research (B) 223 80095 provided by Japan Society for Promoting Science. Authors also would like to express their sincere thanks to Mr. Shoichi Nakashima, Mr.Kenji Komatsu, Miss Sok Yee Yeo, and Dr. Zeli Que for their tremendous efforts for completing test specimen.

## REFERENCES

[1] C.E.Grigorian, T.S.Yang and E.P.Popov: Slotted Bolted Connection Energy Dissipation, *Earthquake Spectra*, Vol.9, No.3, 491-504, 1993.

[2] Anon : Cost-Effective Energy Dissipating Connections, Modern Steel Construction, pp.40-42, February, 1994.

[3] M.D. Symans et al. : Energy Dissipation Systems for Seismic Applications: JOURNAL OF STRUCTURAL ENGINEERING, ASCE, pp.3-21, JANUARY 2008.

[4] S.F.Duff, R.G.Black, S.A.Mahin and M.Blondet : Friction Damped-Energy Dissipating Timber Connection, Proceedings of 5th World Conference on Timber Engineering, Lausanne Presses Polytechniques et Universitaires Romandes, Montreux, Switzerland. Vol. 1, pp.361-368, 2005.

[5] Yoshikazu Araki, Toshiki Endo and Manami Iwata : Feasibility of improved slotted bolted connection for timber moment frames, Journal of Wood Science, 57, pp.247-253, 2011.

[6] Kohei Komatsu and Shoichi Nakashima : Development of much stiffer and rich ductile glulam portal frame which can be easily repaired and restored after being attacked by devastating earthquakes. (1) Development of joint method and static evaluation of the performance, Summary of Technical Papers of Annual Meeting of AIJ, Toukai, Structure -3, 531–532, 2012.(in Japanese)

[7] Kohei Komatsu, Shoichi Nakashima and Akihisa Kitamori : Development of Ductile Moment-Resisting Joint Based on a New Idea for Glulam Portal Frame Structures, *Proceedings of WCTE2012, Session 19, Connections 7*,pp.156-161, Auckland, NZ, 2012.

[8] Sukenobu Tani, Setsuro Nomura, Tomoya. Nagasawa and Akira. Hiramatsu, "Re- storing Force Characteristics of Reinforced Concrete Aseismatic Elements (Part 1): Restoring Force Characteristics and Modellization," *Transactions of Architectural Institute of Japan*, Vol. 202, 1972, pp. 11-19. (in Japanese)

[9] Walter Ramberg and William R. Osgood : Description of Stress-Strain Curves by Three Parameters, National Advisory Committee for Aeronautics, Technical Note No.902, Washington, July, 1943.

[10] ANON : SNAP 6,0,0,8 KOZO SYSTEM, 2012

[11] ANON : Design Manual on Timber Joints by Lagscrewbolts, p.48, Japan Lagscrewbolt Society, 2012. (in Japanese)

[12] AIJ Sub-Committee for Timber Structures: Standard for Structural Design of Timber Structures – Allowable stress and allowable strength design method-, Architectural Institute of Japan, Maruzen, the 4th edition, 1st print, 2006.

[13] Satoru Murakami, Akihisa Kitamori and Kohei Komatsu: Reinforcement on Column-Beam joint with large-cross-section lumber by full-threaded screws, Summary of Technical Papers of Annual Meeting of AIJ, Toukai, Structure -3, 527–528, 2012. (in Japanese)